53rd AIAA/ASME/ASCE/AHS/ASC Structures, Structural Dynamics and Materials Conference
20th AI
23 - 26 April 2012, Honolulu, Hawaii

AIAA 2012-1423

Fracture Analysis of Thick Adhesive Joints for Wind Turbine Blades

Kyeongsik Woo[1] and Wei Wang[2]
Chungbuk National University, Cheongju, Chungbuk, 361-763, Korea

and

Matt Peterson[3], Douglas S. Cairns[4], and John F. Mandell[5]
Montana State University, Bozeman, MT 59717, USA

In this study, the fracture behavior of thick adhesive lap shear joint was numerically investigated. The joint configuration consisted of E-glass/epoxy laminated adherends and Epoxy adhesive in between. Both the adhesive and adherend were modeled using plane strain elements, and cohesive elements were inserted between every element in the overlapping region of the adhesive where the fracture was expected to occur. For the cohesive elements, triangular shape traction-separation relation was selected and the cohesive properties obtained from tests were used. Various adhesive thicknesses and overlap lengths were considered and the effect of boundary conditions was addressed. Results indicated that the analysis predicted well both the crack propagation history and the apparent joint strength.

Nomenclature

E	=	Young's modulus of adhesive
E_{11}, E_{22}	=	Young's moduli of glass fabric composite
F	=	applied force
G_{12}	=	shear modulus of glass fabric composite
G_{Ic}, G_{IIc}	=	mode 1 and mode 2 fracture energy of adhesive
K_{eff}	=	initial stiffness of traction-separation relation
L	=	overlap length
T_{Nmax}, T_{Tmax}	=	maximum normal and tangential traction stresses
t_{adh}	=	adhesive thickness
u, v	=	displacements
W	=	width of joint specimen
Z	=	total length of joint specimen
ν	=	Poisson's ratio of adhesive
ν_{12}	=	Poisson's ratio of glass fabric composite
σ_{max}	=	major principal stress
τ_{app}	=	apparent joint strength

I. Introduction

Adhesive joint failure in wind turbine blades has been a persistent industry problem and become an issue of increasing importance as the blade size has increased. Typical blade joints use paste adhesives several millimeters thick, of varying geometry. They can be expected to experience significant static and fatigue loads under

[1] Professor, School of Civil Engineering. Senior AIAA Member, kw3235@chungbuk.ac.kr.
[2] Graduate Research Assistant, Department of Civil Systems Engineering.
[3] Graduate Research Assistant, Department of Mechanical and Industrial Engineering.
[4] Professor, Department of Mechanical and Industrial Engineering.
[5] Professor, Department of Chemical and Biological Engineering.

various environmental conditions over their service life. The limited data available for joints of this class with metal or composite adherends indicate significant sensitivity to adherend properties and surface preparation, adhesive composition (chemistry, additives, mixing, curing), adhesive thickness, temperature, and moisture, as well as joint geometry. The variability of joint strength can be greater than that of typical laminates due to a higher sensitivity to flaws such as porosity in the adhesive, poor mixing, unbonded areas or poor dimensional control.

Joint design and structural adhesives technology have been the subjects of many studies. References [1-4] explore many of the adhesive joint parameters for general aircraft, which are also of relevance to wind blades in many instances. The strengths of lap-shear and many other joint designs for relatively brittle adhesives are dominated by stress concentrations at corners and edges of the adhesive, rather than an average stress condition across the joint[5-6]. The interpretation of test results must consider the stress concentration problem, even if strength data are represented by the average stress across the joint. Because of this problem, the failure of joints is often considered in a fracture mechanics context, with artificial or assumed cracks[7-10].

Failure modes in adhesive joints are broadly represented in the literature as cohesive within the adhesive layer, or interfacial between the adhesive and the adherend; both may be dominated by either shearing or peeling stresses depending on factors such as adherend thickness[1]. Failure may also occur away from the joint in the adherend, or in the adherend adjacent to the adhesive. Delamination between plies, particularly the first ply below the adhesive, has been reported as a failure mode for composite adherends[1]. Lap shear tests have been the basis for most of the cited literature studies.

In this paper, the fracture behavior of lap shear joint with thick adhesive was studied by finite element analysis. The adhesive and adherend layer of lap-shear joint configuration was modeled using plane strain elements. To predict the fracture behavior of the joint, cohesive elements were inserted between every element in the adhesive layer. The apparent strengths of the joint and the crack propagation history were predicted and compared to the test results. Various adhesive thicknesses and overlap lengths was considered and the effect on the fracture behavior was systematically investigated.

II. Analysis

A. Configuration

Figure 1 shows the configuration of the notched adhesive lap shear joint analyzed in this study. This was the specimen configuration tested in Reference [11], which was fabricated as a sandwich with the cured laminate adherends on the outside and the epoxy adhesive layer between; specimens were machined as strips, with notches then machined to provide the specified overlap length. The diameter of the mill cuts was 6.4 mm and the 1mm at the bottom of adhesive layer was left. The thickness of adherend layers was 5 mm, the width of the specimen (W) was 25 mm, and the total length of the specimen (Z) was 200 mm. In this study, the adhesive thicknesses (t_{adh}) considered were 3.25 mm, 6.5 mm, and 9.75 mm, and the overlap lengths (L) were 12.7 mm and 25.4 mm.

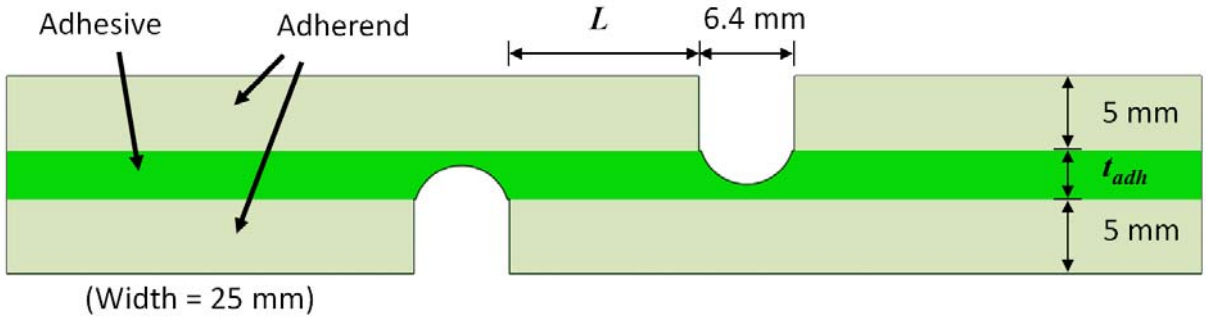

Figure 1. Notched adhesive lap-shear joint configuration.

B. Finite element modeling

Figure 2 shows an example of finite element mesh for the case when L = 12.5 mm and t_{adh} = 3.25 mm. In this study, a commercial finite element analysis software ABAQUS was used for the analysis. The configuration including the adhesive and the adherend was modeled using plane strain elements (CPE4/CPE3). As can be seen in

the figure, the adhesive layer between the notches where the failure was expected to occur was highly refined and most elements were concentrated. In this region, "zero-thickness" cohesive elements (COH2D4) were inserted between every element. To give more freedom in the crack propagation direction, unstructured triangular elements were used in this region. Assuming the crack would initiate and propagate only in the adhesive layer, no cohesive element was added in the adherend region. The number of total regular elements was 42,326 and the number of cohesive elements was 42,098 for the case shown in this figure. Increased number of elements were used for the meshes for configurations with thicker adhesive and longer overlap lengths.

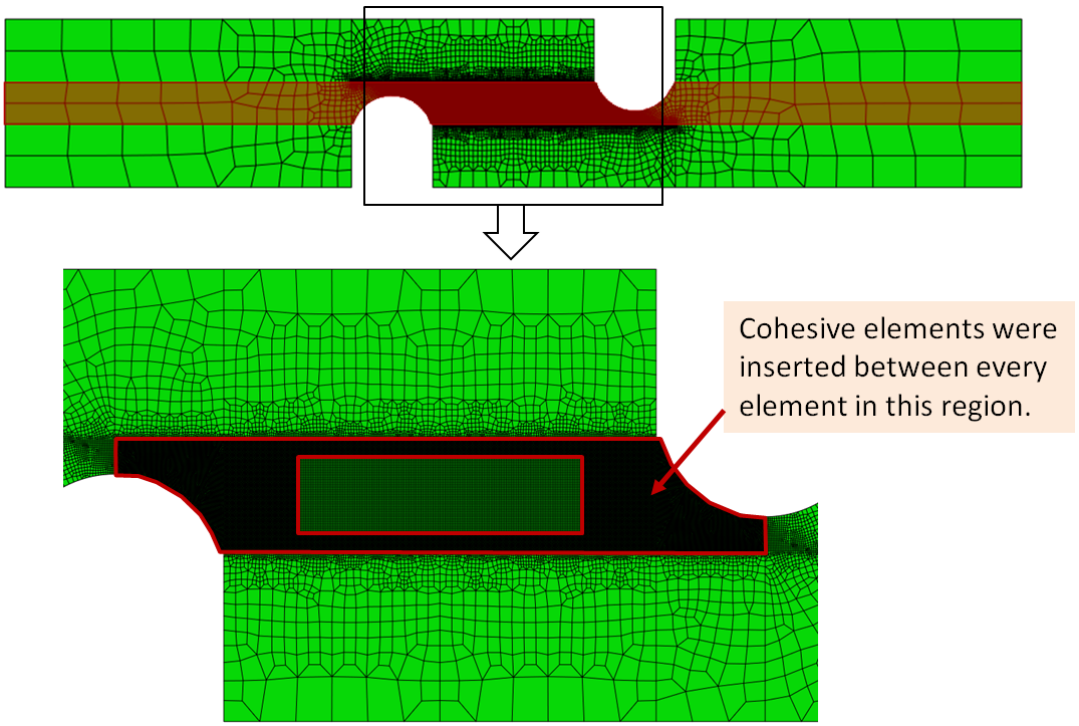

Figure 2. Example finite element mesh and insertion of cohesive elements.

C. Material properties

As explained in Figure 1, the adhesive joint consisted of the epoxy adhesive layer and the adherend laminates. The adherend laminates were made by stacking 5 layers of E-glass/epoxy stitched unidirectional fabric. The material properties of the adherend laminates were: E_{11} = 41.7 GPa, E_{22} = 14.1 GPa, ν_{12} = 0.263, and G_{12} = 4.7 GPa. The property of adhesive layers was obtained from test[11]. Figure 3 shows the tensile stress-strain curve for the epoxy adhesive resin which exhibited a large amount of nonlinearity. In the analysis, the adhesive was assumed to behave elasto-plastically. The initial modulus (E) and Poisson's ratio (ν) were 3.4 GPa and 0.35, respectively. The yield stress was 51.5 MPa and the ultimate stress was 62.5 MPa.

D. Traction-separation relation

The accuracy of predicting the crack propagation behavior is mainly dependent on the traction-separation relation of the cohesive elements (e.g., Refs. [12-14]). In this study, a typical triangular shape traction-separation relation was used. The cohesive mode I fracture parameters of the adhesive material were G_{Ic} = 0.7 N/mm and T_{Nmax} = 62.5 MPa, which were obtained from tests[11]. The test to obtain the mode II parameters was not performed. The values used in the analysis were G_{IIc} = 1.0 N/mm and T_{Tmax} = 50 MPa. A simple power law was used for the mixed mode behavior. Since a large number of cohesive elements were used, the structure can have significant added compliance. To minimize this effect, the convergence study was performed to determine the initial stiffness (K_{eff}) of the traction-separation relation. It was found that for the currently considered materials and finite element meshes, the initial stiffness of $K_{eff} = T_{Nmax} / 10^{-5}$ MPa/mm produced the reasonably well converged results while not slowing

down the computation process too much. Also, a small amount of artificial damping was added to the cohesive elements to stabilize the solution procedure.

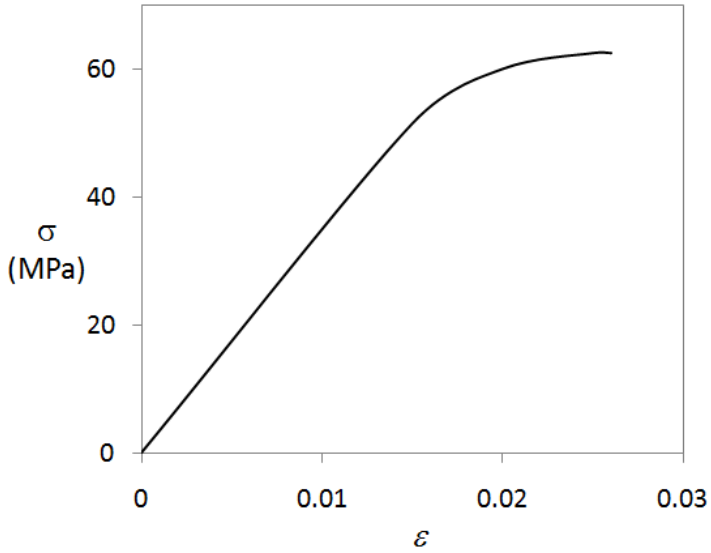

Figure 3. Tensile stress-strain curve for the epoxy adhesive.

E. Boundary conditions

Figure 4 shows the load and boundary conditions used. In the figure, the thick lines indicate the grips. The load was applied by specifying displacement. The amount of applied load was then calculated from the reaction nodal forces. It was reported in the test that the joint specimen showed lateral movement[11]. To address this effect, two types of boundary conditions were considered. The right side grip was assumed to move freely in the lateral direction in BC1, while it was constrained in BC2. The grip of the left side was assumed to be fixed in both cases.

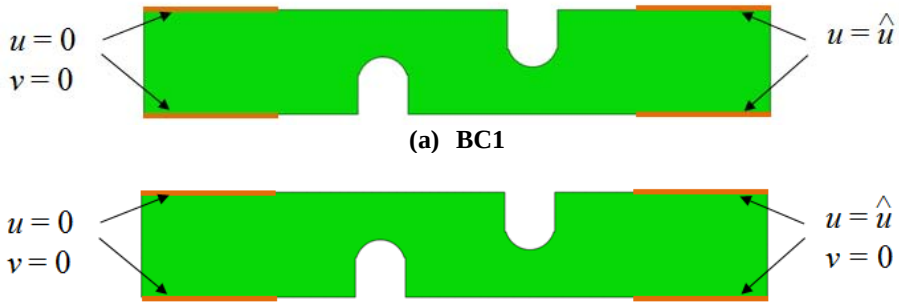

(a) BC1

(b) BC2

Figure 4. Load and boundary conditions applied.

III. Results and Discussion

A. Crack propagation history

Figure 5 shows the crack propagation history for the lap shear joint with the overlap length L = 12.7 mm and the adhesive thickness t_{adh} = 3.25 mm when the boundary condition BC1 was used. The circled number marks the major events during the crack propagation process; in Figure 5(b) the major principal stress distribution was plotted for the corresponding stage. From the figure, the crack initiation and propagation history of the thick adhesive lap shear joint can be divided as follows.

(1) Crack initiated on the left-side circular mill-cut adhesive surface, and propagated to the upper adhesive-adherend interface.
(2) Crack hit the upper interface, then propagated along the interface line.
(3) Another crack initiated at the opposite mill-cut adhesive surface.
(4) The upper interface crack propagated completely through the bondline.

The initial crack opening and propagation occurred predominantly in mode I. When the crack hit the interface and started to follow the bondline, it became a mixed-mode problem. As the crack propagated along the bondline, the mode II component increased gradually and the crack growth slowed. Then, a new crack started to open at the opposite side and propagated similarly. Finally the crack started from the left hand side propagated completely through the upper bondline separating the upper adherend from the structure. The crack started from the right hand side propagated only partially through the lower bondline.

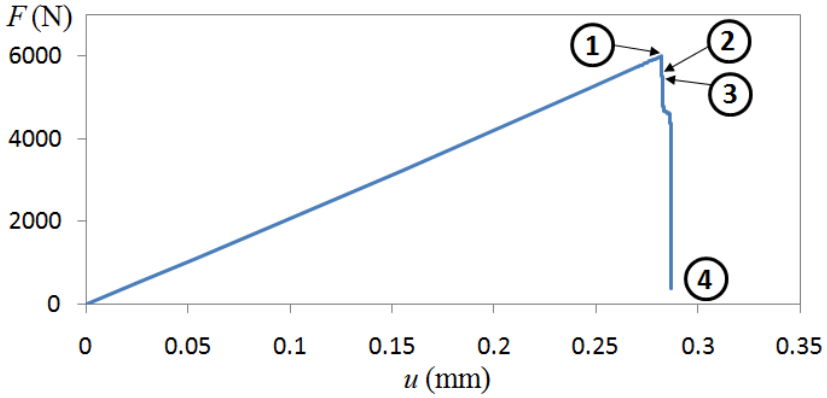

(a) Load-displacement curve

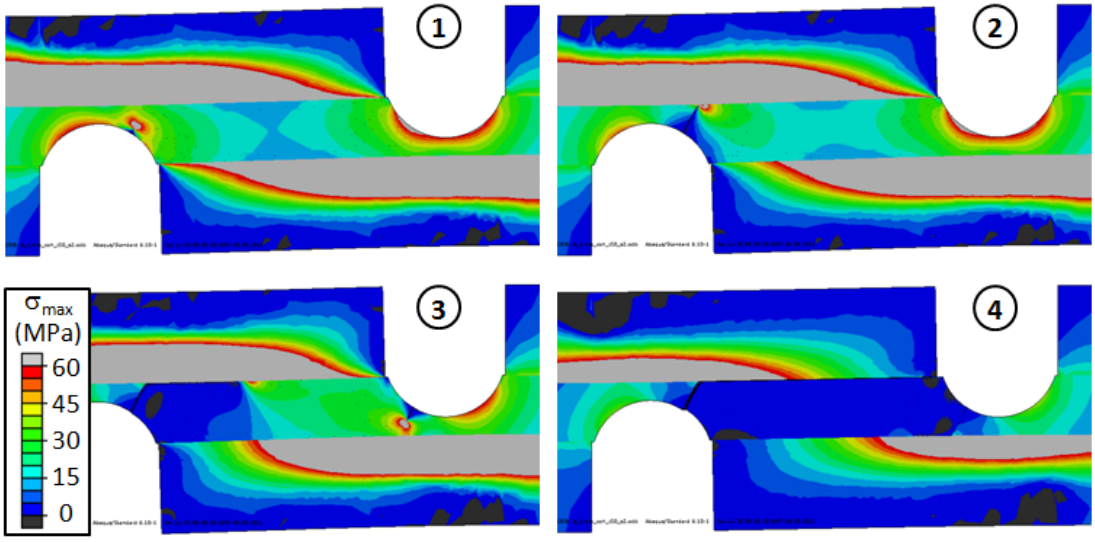

(b) Major principal stress distribution snap shot

Figure 5. Crack propagation history with BC 1. (t_{adh} = 3.25 mm, L = 12.7 mm)

B. Effect of boundary condition

Figure 6 compares the load versus displacement curves of the joints analyzed with different boundary conditions. In BC2, the structure appeared to be much stiffer since the lateral movement at the grip was constrained. This constraining reduced the amount of bending deformation of the joint and, as a result, the crack opening at the mill-cut round surface occurred at much higher load. The global crack propagation pattern was similar to the case of BC1.

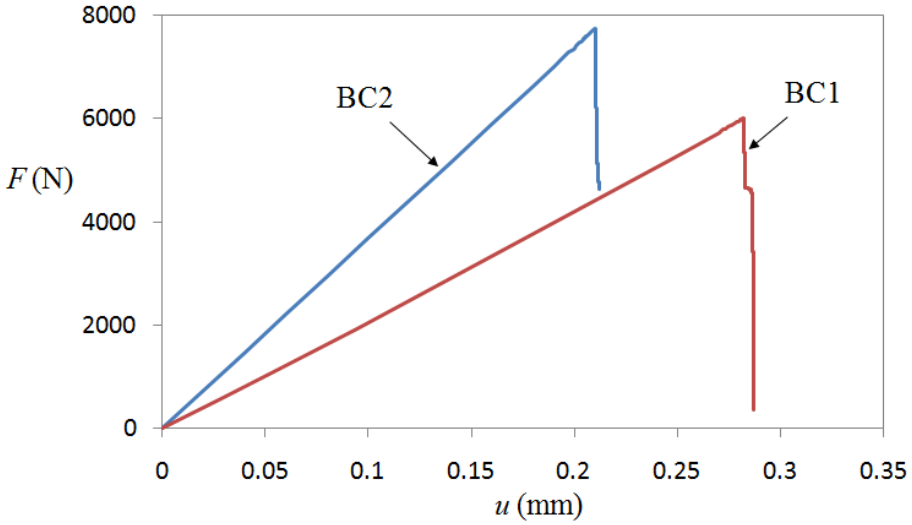

Figure 6. Comparison of load-displacement curves of adhesive joint with different boundary conditions. (The boundary conditions of BC1 and BC2 were defined in Figure 4.)

C. Strength prediction

From the peak load values, the 'apparent' joint strength was calculated. The apparent joint strength was defined as

$$\tau_{app} = \frac{F}{W \times L} \tag{1}$$

where F, W, and L denoted the applied load, the joint width, and the overlap length, respectively.

Table 1 summarizes the joint strength values for various adhesive thicknesses and overlap lengths. In the table the numerically calculated strengths of thee difference adhesive thicknesses were compared with the test results[11] when the overlap length (L) was 25 mm. When the overlap length was 12.5 mm, only the case of t_{adh} = 3.25 mm was listed since the test results were not available for other adhesive thicknesses. Figure 7 shows the results graphically when the overlap length was 25 mm. As one can see, the predicted joint strengths agreed well with the test results. The analysis results with the different boundary conditions bounded the test results indicating that better strength prediction would be possible if the actual test conditions were more closely simulated in the analysis.

Table 1. Comparison of numerically calculated and experimentally obtained joint strengths for the thick adhesive lap shear joint.

L (mm)	t_{adh} (mm)	τ_{app} (MPa)		% diff.
		Test	Analysis	
12.5	3.25	21.6	19.17 (BC1) 24.36 (BC2)	-11.3 12.8
25	3.25	14.1	11.66 (BC1) 15.60 (BC2)	-17.3 10.6
	6.5	10.2	8.94 (BC1) 13.4 (BC2)	-12.4 31.4
	9.75	8.81	7.28 (BC1) 11.1 (BC2)	-17.4 26.0

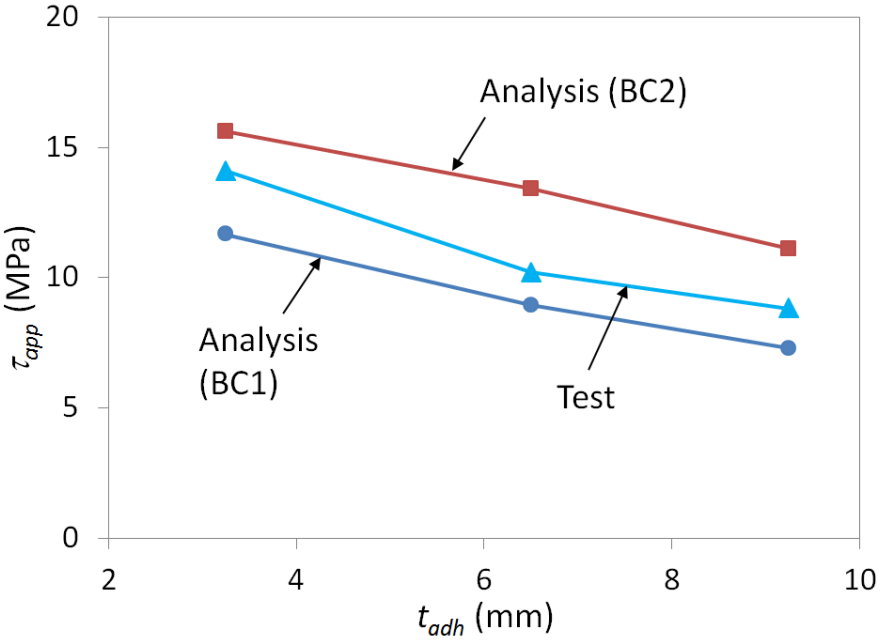

Figure 7. Variation of apparent joint strengths versus adhesive thickness (*L* = 25 mm).

IV. Conclusion

In this study, the fracture strength of thick adhesive lap shear joint was calculated by numerical simulations. The joint configuration consisted of E-glass/epoxy laminated adherends and Epoxy adhesive in between. Plane strain condition was assumed and the cross-section of both the adhesive and adherend was modeled by 2-dimensional elements. Then cohesive elements were inserted between every element in the overlapping region of the adhesive where the fracture was expected to occur. For the cohesive elements, triangular shape traction-separation relation was used. The cohesive properties obtained from tests were used and the initial stiffness was selected after a series of numerical tests. Two types of boundary conditions were considered.

Results indicated that the analysis predicted well both the crack propagation history and the apparent joint strength. It was found that the crack initiated at the circular mill-cut surface of the adhesive, propagated toward the adhesive-adherend interface, continued along the bondline, and separated one side of the interface completely. The calculated apparent joint strengths with two different boundary conditions bounded the test results with good agreement for all cases with different adhesive thicknesses.

References

[1]Tomblin, J., Harter, P., Seneviratne, W., and Yang, C., "Characterization of Bondline Thickness Effects in Adhesive Joints," *J. Composites Tech. and Res.*, 24:80-92, 2002.

[2]Tomblin, J., Yang, C. and Harter, P, "Investigation of Thick Bondline Adhesive Joints," FAA Report DOT/FAA/AR-01/33, June, 2001.

[3]Tomblin, J., Seneviratne, W., Escobar, P. and Yap, Y., "Shear Stress-Strain Data for Structural Adhesives," FAA Report DOE/FAA/AR-02/97, November, 2002.

[4]Tomblin, J., Seneviratne, W., Escobar, P. and Yap, Y., "Fatigue and Stress Relaxation of Adhesives in Bonded Joints," FAA Report DOE/FAA/AR-03/56, October, 2003.

[5]Goland, M. and Reissner, E., "The Stresses in Cemented Joints," *J. Appl. Mechanics*, 11:17-27, 1944.

[6]Hart-Smith, L.J., "Developments in Adhesives 2," Kinloch, A.J., ed., *Applied Science Publications*, London, 1981.

[7]Kinloch, A.J., and Osiyemi, S.O., "Predicting the Fatigue Life of Adhesively-Bonded Joints," *J. Adhesion*, 43:79-90, 1993.

[8]Curley, A.J., Hadavinia, H., Kinloch, A.J. and Taylor, A.C., "Predicting the Service Life of Adhesively - Bonded Joints," *Inter. J. Fracture*, 103:41-69, 2000.

[9]Sancaktar, E., "Fracture Aspects of Adhesive Joints: Material, Fatigue, Interphase and Stress Concentrations," *J. Adhesion Sci. and Tech.*, 9:119-147, 1995.

[10]Ripling, E.J., Mostovoy, S. and Patric, R.L., "Application of Fracture Mechanics to Adhesive Joints," Adhesion, ASTM STP 360, ASTM, Phil., p.5, 1963.
[11]Mandell, J.F., Samborsky, D.D., Agastra, P., Sears, A.T., and Wilson, T.J., "Analysis of SNL/MSU/DOE Fatigue Database Trends for Wind Turbine Blade Materials," SNL Report SAND2010-7052, 2010.
[12]Xu, X.P. and Needleman A., "Void nucleation by inclusions debonding in a crystal matrix," *Model Simul Mater Sci Engng*, 1:111–32, 1993.
[13]Tvergaard, V. and Hutchinson, J.W., "The relation between crack growth resistance and fracture process parameters in elastic–plastic solids," *J Mech Phys Solids*, 40:1377–97, 1992.
[14]Camacho, G.T. and Ortiz, M., "Computational modelling of impact damage in brittle materials," *Int J Solids Struct*, 33:2899–938, 1996.